

Diquark confinement in an extended NJL model[†]

G. Hellstern¹, R. Alkofer and H. Reinhardt

*Institute for Theoretical Physics
 Tübingen University
 Auf der Morgenstelle 14
 D-72076 Tübingen, Germany*

Abstract

In a Nambu–Jona-Lasinio model supplemented with an infrared cutoff in addition to the ultraviolet cutoff we study the issue whether diquarks are confined when the model is extended beyond the rainbow-ladder approximation. The gap equation, obtained in a truncation scheme motivated via a nontrivial quark-gluon vertex function, is solved to determine the constituent quark mass if chiral symmetry is spontaneously broken. In a second step, the Bethe-Salpeter equations for mesons and diquarks beyond ladder approximation are derived, taking care to preserve Goldstone’s theorem in the pion channel. While the obtained masses of pseudoscalar and vector mesons are only moderately shifted compared to the values in ladder approximation, we observe that scalar diquarks disappear from the physical spectrum and therefore are confined. For axialvector diquarks we observe indications, that the same mechanism may also work, but the NJL model allows no conclusive answer in this channel.

Key words: Diquark; Meson; NJL model; Confinement; Bethe-Salpeter equation.

PACS: 12.38.Aw; 12.39.-x; 14.65.Bt; 12.40.Yx; 11.30.Rd.

[†] Supported by BMBF under contract 06TU888 and Graduiertenkolleg “Hadronen und Kerne” (DFG Mu705/3).

¹ E-mail: Gerhard.Hellstern@uni-tuebingen.de

1 Introduction

Although QCD is believed to be the theory of strong interactions hadron properties have not yet been calculated from this underlying fundamental theory. Thus it proves helpful to develop effective theories including the characterizing features of QCD as e.g. asymptotic freedom, confinement and chiral symmetry including its breaking pattern. A model solely built on chiral symmetry and leaving aside the question of confinement and the transition to the perturbative region is the Nambu–Jona-Lasinio (NJL) model [1], formulated with quarks as elementary degrees of freedom interacting locally. Modeling the gluon sector to incorporate quark confinement is done in the Global Color Model (for a recent review see [2]). Both approaches, due to their construction principles, are able to describe the lowest lying meson states quite reasonably. Baryons then emerge as solitons of the effective meson theory [3, 4]. However, the modeled gluon interaction also gives rise to quark-quark correlations, leading to a picture of baryons as diquark-quark bound states [5, 6] (a hybrid model combining the soliton with the bound state picture has been developed in ref. [7]).

Although diquarks have many appealing phenomenological aspects (see e.g. [8]) and are useful tools to parametrize unknown and/or complicated structures, there remains the question whether diquarks are realized in nature. Diquarks as constituents in a baryon have to be necessarily in a color antitriplet state to build a colorless baryon when interacting with a third quark. On the other hand, an antitriplet state is forbidden as an asymptotic state in a presumably confining theory like QCD. When the lowest lying diquark states (scalar and axialvector) are evaluated in the NJL model in ladder approximation they are not confined. Also in the Global Color Model, which leads to quark confinement if certain effective quark-quark interactions (which basically have to provide enough interaction strength in the infrared) are used, diquarks are predicted to be “observable” particles [9].

In ref. [10] it has been conjectured that this fact is due to the commonly applied rainbow-ladder approximation and diquark confinement can be obtained when the quark Dyson-Schwinger equation as well as the diquark Bethe-Salpeter equation are considered beyond rainbow and ladder approximation, respectively. While these studies have been performed in the Munczek–Nemirovsky model [11], assuming an especially simple form for the gluon propagator¹, it has also been claimed that the observed feature of diquark confinement is generic and in particular independent of the gluon propagator. Redoing the calculations of [10] with a realistic gluon propagator (e.g. with the ones reported in

¹In all these studies it is assumed that the quark-quark interaction is given solely by the gluon propagator despite the fact that this is not quite correct in a non-Abelian gauge theory. E.g. ghosts invalidate this identification and an infrared diverging ghost propagator drastically alters this picture [12].

ref. [13]) would be a very complicated task. We therefore want to test the conjecture of diquark confinement in a model, which assumes a quite different but also simplified gluon dynamics: Whereas in the Munczek–Nemirovsky model the gluon propagator is a delta function in momentum space leading to a constant propagator in coordinate space, in the NJL model the gluon propagator is assumed to be a delta function in coordinate space, leading to a constant propagator in momentum space. When working with a nonrenormalizable theory, divergent integrals have to be regularized, leaving the cutoff finite. We will use the proper-time method suggested in [14], i.e. besides the usual UV cutoff also an infrared cutoff is introduced to remove unphysical quark thresholds from correlation functions and therefore mimicing quark confinement.

The paper is organized as follows: In the next section we solve the gap equation (quark Dyson-Schwinger equation) beyond rainbow approximation; in section 3 we show how the kernel of the meson and diquark Bethe-Salpeter equation have to be consistently constructed to preserve Goldstone’s theorem in the pion channel. The solution of the Bethe-Salpeter equations for pions (0^-), vector mesons (1^+), scalar (0^+) and axialvector diquarks (1^-) beyond ladder approximation are presented and discussed. After summarizing our results we will close with an outlook. In the appendices we discuss the elimination of thresholds in the generalized proper-time scheme and N_c –counting beyond ladder approximation.

2 Gap equation beyond rainbow approximation

In Minkowski space² the Dyson-Schwinger equation, determining the dressed quark propagator is given by

$$\begin{aligned} iS^{-1}(p) &= \not{p} - \Sigma(p) \\ \Sigma(p) &= m_0 + g^2 i \int \frac{d^4 k}{(2\pi)^4} D_{\mu\nu}(p-k) \frac{\lambda^a}{2} \gamma^\mu S(k) \Gamma_\nu(p, k) \frac{\lambda^a}{2}. \end{aligned} \quad (1)$$

It connects the quark propagator $S(p)$ with the gluon propagator $D_{\mu\nu}(p)$ and the quark-gluon vertex function $\Gamma_\nu(p, k)$. The generators of color SU(3), the Gell-Mann matrices, are denoted by $\lambda^a/2$. In the NJL model the gluon propagator is assumed to be

$$g^2 D_{\mu\nu}(p) \equiv G g_{\mu\nu}, \quad (2)$$

leading to an effective, nonrenormalizable local quark-quark interaction governed by the coupling strength G . When furthermore the quark-gluon vertex function is substituted

²All calculations are done in Minkowski space; a Wick rotation is performed only to evaluate the final integrals. We furthermore assume exact flavor SU(2) symmetry and suppress all explicit flavor indices.

$$\Sigma(p) = m_0 + \text{[rainbow diagram]} + \text{[vertex correction diagram]}$$

Figure 1: The quark Dyson-Schwinger equation including the nontrivial quark-gluon vertex function is shown. Note, that due to the ansatz of the gluon propagator (eq. (2)) the gluon lines are momentum independent and merely represent the color flow through the diagrams.

by its perturbative expression (γ_μ) one ends up with the quark Dyson-Schwinger equation of the NJL model in mean field or rainbow approximation. As suggested in ref. [10], a minimal way to go beyond rainbow approximation is to include the vertex correction to first order in G :

$$\frac{\lambda^a}{2}\Gamma_\mu(k, p) = \frac{\lambda^a}{2}\gamma_\mu + Gi \int \frac{d^4 l}{(2\pi)^4} D_{\rho\nu}(p-l) \gamma^\nu \frac{\lambda^b}{2} S(l+k-p) \gamma_\mu \frac{\lambda^a}{2} S(l) \gamma^\rho \frac{\lambda^b}{2} \quad (3)$$

$$= \frac{\lambda^a}{2} \left[\gamma_\mu + \frac{-1}{6} G \gamma_\mu \Gamma^L((k-p)^2) \right]. \quad (4)$$

The part of the vertex function $\Gamma^L((k-p)^2)$, describing the dressing of the perturbative quark-gluon vertex is given by

$$\gamma_\mu \Gamma^L((k-p)^2) = i \int \frac{d^4 l}{(2\pi)^4} \gamma_\nu S(l+k-p) \gamma_\mu S(l) \gamma^\nu. \quad (5)$$

leading to the quark Dyson-Schwinger equation

$$\begin{aligned} \Sigma(p) = m_0 &+ \frac{4}{3} Gi \int \frac{d^4 k}{(2\pi)^4} \gamma_\mu S(k) \gamma^\mu \\ &+ \frac{-2}{9} G^2 i \int \frac{d^4 k}{(2\pi)^4} \gamma_\mu S(k) \gamma^\mu \Gamma^L((k-p)^2). \end{aligned} \quad (6)$$

Throughout the paper we will denote factors, arising from the color structure by “**sans serif**” letters. In fig. (1) the quark Dyson-Schwinger equation beyond rainbow approximation is shown. Note, the gluon lines appearing in the Feynman diagrams are given by eq. (2) and are therefore momentum independent.

Here and in the following we regularize loop integrals in a generalized proper-time scheme,

$$\frac{1}{N^n} = \frac{1}{(n-1)!} \int_0^\infty ds s^{n-1} \exp(-sN) \rightarrow \frac{1}{(n-1)!} \int_{\frac{1}{\Lambda^2}}^{\frac{1}{\mu^2}} ds s^{n-1} \exp(-sN), \quad (7)$$

where N^n is the denominator of a Wick rotated loop integral after introducing the appropriate Feynman parameter integral and performing a corresponding momentum shift.

	Rainbow, $O(G)$		Beyond Rainbow, $O(G^2)$	
	$m_0 = 0$	$m_0 = 0.017$	$m_0 = 0$	$m_0 = 0.017$
$\mu = 0.1$	0.3873	0.400	0.4194	0.4295
$\mu = 0.2$	0.3873	0.400	0.4194	0.4297

Table 1: *The solution of the gap equation in rainbow ($O(G)$) and beyond rainbow approximation ($O(G^2)$) is shown. We used parameters, which are fixed in the standard NJL model: The chosen set ($\Lambda = 0.630 \text{ GeV}$, $G = 184.18 \text{ GeV}^{-2}$, $m_0 = 0.017 \text{ GeV}$) lead to $M = 0.4 \text{ GeV}$ and to the pionic observables $m_\pi = 0.140 \text{ GeV}$ and $f_\pi = 0.093 \text{ GeV}$, when the dominant amplitude of the pion (see eq. (13) is considered) [15]. In the chiral limit the same parameters are used, but $m_0 = 0$. All masses and scales are given in units of GeV.*

As has been shown in ref. [14] any nonvanishing infrared cutoff μ (with $\mu \ll \Lambda$, where Λ is the ultraviolet cutoff) removes unphysical quark thresholds from correlation functions and therefore simulates quark confinement in a crude way, for details we refer to Appendix A. Note, however, although this prescription allows to investigate correlation functions at external momenta $P^2 > 4M^2$, i.e. above the “pseudo”threshold, without opening the unphysical decay channel, this quark confinement mechanism is certainly too naïve to explain physics far above the pseudothreshold. Due to the gauge invariance of the proper-time regularization, we especially find that the vertex correction is purely longitudinal (see eq. (4)). We furthermore observe that the vertex correction can be very well approximated by a simple dipole

$$\Gamma^L(Q^2) \sim \frac{a}{(Q^2 + b)^2}, \quad (8)$$

with coefficients $a(M, \Lambda, \mu)$ and $b(M, \Lambda, \mu)$ obtained by a χ^2 -fit to the regularized result of eq. (5) which obviously depend on Λ , μ and M . Using the effective parametrization of the quark-gluon vertex correction (8) in eq. (6) one finally ends up with the gap equation determining the constituent quark mass ³:

$$\begin{aligned} M = m_0 &+ \frac{1}{16\pi^2} \cdot \frac{4}{3} \cdot 4M^2 G \left(\Gamma(-1, M^2/\Lambda^2) - \Gamma(-1, M^2/\mu^2) \right) \\ &+ \frac{1}{16\pi^2} \cdot \frac{-2}{9} \cdot 4MaG^2 \left(\int_0^1 dx (1-x) \frac{1}{Y^2} (\exp(-Y^2/\Lambda^2) - \exp(-Y^2/\mu^2)) \right), \\ Y^2 &= (1-x) \cdot b + xM^2. \end{aligned} \quad (9)$$

While the first line of eq.(9) is the familiar mean field result, the second line arises from the vertex correction. Although the term induced by the vertex correction leads to a

³ $\Gamma(n, x)$ denotes the incomplete Gamma function arising in the proper-time regularization scheme.

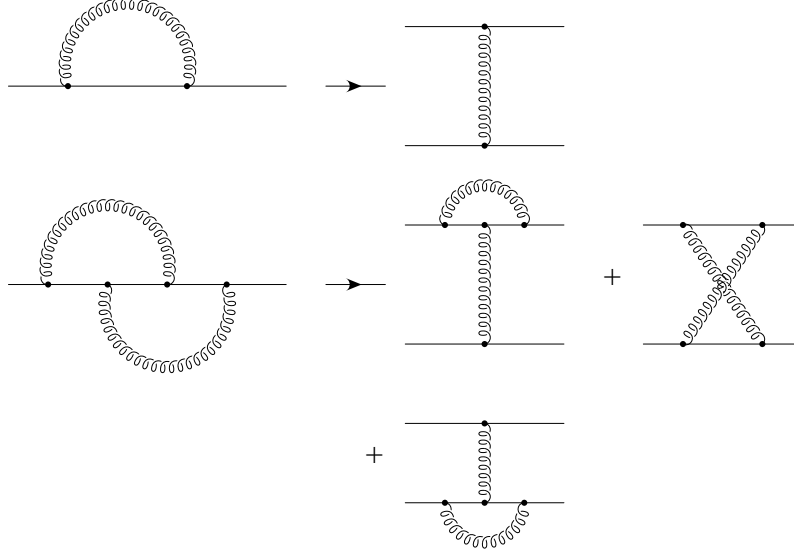


Figure 2: In this figure we display how the kernel of the meson Bethe-Salpeter equation is obtained from the quark self-energy diagrams by cutting all possible internal quark lines. See also fig.(1) of ref. [10].

momentum dependent quark mass we assume that the momentum dependence at low energies is weak and it is therefore legitimate to work with $\Sigma(p^2) \equiv M = \text{const.}$ in eq. (6). The gap equation (9) can be solved by taking the dependence of the dipole coefficients $a(M, \Lambda, \mu)$ and $b(M, \Lambda, \mu)$ on M properly into account. Our results are displayed in table (1). It is seen, that the vertex correction is repulsive, leading to slightly larger constituent quark masses. When doing the calculation with different values of the infrared cutoff μ , we find that the results are quite insensitive on μ , as long as there is enough phase space available i.e., the condition $\mu \ll \Lambda$ is fulfilled.

3 Bethe-Salpeter equation for mesons and diquarks

The Bethe-Salpeter equation describing mesons as quark-antiquark bound states is written as

$$\Phi_M(P, p) = \int \frac{d^4 k}{(2\pi)^4} K_M(k, p; P) (S(k + \tfrac{1}{2}P) \Phi_M(P, k) S(k - \tfrac{1}{2}P)). \quad (10)$$

In ladder approximation the kernel $K_M(k, p; P)$ reduces itself to a momentum independent contact interaction, reflecting the local quark-quark interaction of the NJL model. It is well known, and can be proved quite easily, that the ladder approximation preserves Goldstone's theorem: When the constituent quark mass obtained from the gap equation (eq. (9) without the vertex correction) in the chiral limit is used in eq. (10), one immediately finds massless bound states with quantum numbers of pions (Goldstone bosons),

reflecting spontaneously broken chiral symmetry. Following ref. [10] we construct the kernel of the Bethe-Salpeter equation for mesons in a way which preserves the Goldstone theorem in every order of the truncation scheme: The Bethe-Salpeter kernel follows via the replacement [10]

$$\gamma_\mu S(k) \gamma_\nu \rightarrow \gamma_\mu S(k + \tfrac{1}{2}P) \Phi_M(k, P) S(k - \tfrac{1}{2}P) \gamma_\nu \quad (11)$$

from the quark self-energy $\Sigma(p)$. As it is displayed in fig. (2), this corresponds to cut all internal quark lines in the quark self-energy diagrams, fig. (1), thereby generating the Bethe-Salpeter kernel. Since the diagram in $O(G^2)$ contains three internal quark lines, the Bethe-Salpeter kernel beyond ladder approximation consists of three parts. This prescription leads to the meson Bethe-Salpeter equation

$$\begin{aligned} \Phi_M(P, p) = & \frac{4}{3} G_M i \int \frac{d^4 k}{(2\pi)^4} \gamma_\nu S(k + \tfrac{1}{2}P) \Phi_M(P, k) S(k - \tfrac{1}{2}P) \gamma^\nu + \frac{-2}{9} G_M^2 i \int \frac{d^4 k}{(2\pi)^4} \int \frac{d^4 l}{(2\pi)^4} \times \\ & [\gamma_\nu S(k + \tfrac{1}{2}P) \Phi_M(P, k) S(k - \tfrac{1}{2}P) \gamma_\rho S(l + k - p) \gamma^\nu S(l) \gamma^\rho \\ & + \gamma_\nu S(k) \gamma_\rho S(l + k - p + \tfrac{1}{2}P) \Phi_M(P, l + k - p) S(l + k - p - \tfrac{1}{2}P) \gamma^\nu S(l) \gamma^\rho \\ & + \gamma_\nu S(k) \gamma_\rho S(l + k - p) \gamma^\nu S(l + \tfrac{1}{2}P) \Phi_M(P, l) S(l - \tfrac{1}{2}P) \gamma^\rho]. \end{aligned} \quad (12)$$

By G_M we collectively denote the coupling constants $G_M = \{G_\pi, G_{\rho, \omega}\}$ in the different meson channels. While chiral symmetry forces the choice $G_\pi = G$ (see table (1)), the coupling constant in the vector meson channel can be different from that value. Nevertheless, we use $G_M = G_\pi = G_{\rho, \omega} = G$.

Note that the three terms contributing to the Bethe-Salpeter equation in $O(G_M^2)$ appear with an equal color factor of $-(N_c^2 - 1)/(4N_c^2) = -2/9$, see Appendix B. However, after taking the relevant Dirac traces, the second term of order G_M^2 gets an additional minus sign, making this term repulsive compared to the first and third term which are attractive.

In order to be consistent with the approximation employed in the gap equation, i.e. working with a momentum independent constituent quark mass, we have to neglect the relative momentum of the Bethe-Salpeter amplitudes, thereby using $\Phi(P, p) \equiv \Phi(P)$. For a pion the appropriate Dirac structure of the amplitude is given by

$$\Phi_\pi(P) = \gamma_5 \Psi_{\pi 1}(P) + \gamma_5 \not{P} \Psi_{\pi 2}(P). \quad (13)$$

We therefore consider not only the dominant Dirac structure ($\sim \gamma_5$), but also the subdominant amplitude ($\sim \not{P} \gamma_5$), which is necessary to respect chiral symmetry and which induces significant contributions to pionic observables (for a recent investigation see ref.

[16]). Physically, this is due to a possible $\pi - A_1$ -mixing. In case of vector mesons (ρ, ω) , the dominant transversal Dirac structure of the amplitude reads

$$\Phi_{\rho, \omega}^{\mu}(P) = (\gamma_{\mu} - \frac{P_{\mu} \not{P}}{P^2}) \Psi_{\rho, \omega}(P), \quad P_{\mu} \Phi_{\rho, \omega}^{\mu}(P) = 0. \quad (14)$$

Equivalently one may use

$$\tilde{\Phi}_{\rho, \omega}(P) = \epsilon_{\mu}^{\lambda} \gamma^{\mu} \tilde{\Psi}_{\rho, \omega}(P), \quad \epsilon_{\mu}^{\lambda} P^{\mu} = 0, \quad (15)$$

involving the polarization vector ϵ_{μ}^{λ} ($\lambda = 0, \pm 1$) being orthogonal to the total momentum of the vector meson. A possible subdominant amplitude would correspond to a mixing between vector and tensor mesons, which are known to be absent in the NJL model. Therefore we have to restrict ourselves to the dominant Dirac structure but choose it in a way which incorporates transversality from the very beginning. After inserting the ansätze for the Bethe-Salpeter amplitudes (eq. (13) and eq. (14) or (15)) into eq. (12), and taking appropriate Dirac traces, the Bethe-Salpeter equation can be reduced to a system of two coupled algebraic equations for the pions and to one algebraic equation for the vector mesons, with the generic structure of the inverse propagators of composite mesons

$$[\mathbf{A}(P^2) - \mathbf{1}]_{P^2=M_m^2} \Psi_m(P) = 0, \quad (16)$$

where $M_m = M_{\pi}$ or $M_{\rho, \omega}$. The meson masses are given either by the zero of $\det[\mathbf{A}(P^2) - \mathbf{1}]$ (in the pion channel, where $\mathbf{A}(P^2)$ is a 2×2 matrix) or simply by the zero of eq. (16) (in the ρ, ω channel, where it is just one equation).

In Appendix A we discuss the pion Bethe-Salpeter equation in ladder approximation in order to demonstrate how the confinement mechanism via the infrared cutoff μ works.

The two-loop integrals appearing in eq. (12) are calculated as follows: First we perform one integration (e.g. over the momentum l) and find that the result (“longitudinal” and “transversal” part) can be approximated by dipoles, in analogy to eq. (8); the second integration can then be performed using the dipoles as effective interaction between the quark and antiquark. The final expressions for the different $\mathbf{A}(P^2)$ are rather lengthy and will be explicitly given elsewhere [17].

In order to calculate scalar and axialvector diquarks, the partners of the pseudoscalar and vector mesons, respectively, the Bethe-Salpeter equation has to be modified in the following way. The model independent expression of a diquark Bethe-Salpeter equation can be written as

$$\Phi_D(P, p) = \int \frac{d^4 k}{(2\pi)^4} K_D(k, p; P) (S(k + \frac{1}{2}P) \Phi_D(P, k) S^T(k - \frac{1}{2}P)), \quad (17)$$

where “T” denotes the transposed of the Dirac matrix $S(p)$. As has been shown in ref. [10], each contribution to the diquark kernel $K_D(k, p; P)$ can be obtained with the replacement

$$S(p)\gamma_\mu\frac{\lambda^a}{2} \rightarrow [\gamma_\mu\frac{\lambda^a}{2}S(-k)]^T, \quad (18)$$

from the meson kernel $K_M(k, p; P)$ (eq. (12)) which leads to the diquark Bethe-Salpeter equation

$$\begin{aligned} \Phi_D(P, p) = & \frac{-2}{3}G_D i \int \frac{d^4k}{(2\pi)^4} \gamma_\nu S(k + \tfrac{1}{2}P) \Phi_D(P, k) S^T(-k + \tfrac{1}{2}P) \gamma^{\nu T} + G_D^2 i \int \frac{d^4k}{(2\pi)^4} \int \frac{d^4l}{(2\pi)^4} \times \\ & [\frac{1}{9} \gamma_\nu S(k + \tfrac{1}{2}P) \Phi_D(P, k) S^T(-k + \tfrac{1}{2}P) \gamma_\rho^T S^T(-l - k + p) \gamma^{\nu T} S^T(-l) \gamma^{\rho T} \\ & + \frac{-5}{9} \gamma_\nu S(k) \gamma_\rho S(l + k - p + \tfrac{1}{2}P) \Phi_D(P, l + k - p) S^T(-l - k + p + \tfrac{1}{2}P) \gamma^{\nu T} S^T(-l) \gamma^{\rho T} \\ & + \frac{1}{9} \gamma_\nu S(k) \gamma_\rho S(l + k - p) \gamma^\nu S(l + \tfrac{1}{2}P) \Phi_D(P, l) S^T(-l + \tfrac{1}{2}P) \gamma^{\rho T}], \end{aligned} \quad (19)$$

with $G_D = \{G_{0+}, G_{1-}\}$. To match our result in the scalar diquark channel (when only the dominant Dirac structure is considered) with the ones obtained in a ladder NJL calculation [15] we choose $G_{0+} = 2/3G$. To simplify comparison, in the axialvector channel we use $G_{1-} = 2G$, thereby obtaining in ladder approximation the same masses for axialvector diquarks and vector mesons.

When comparing the diquark Bethe-Salpeter equation with the one for mesons, the most striking difference are the different color factors in eq.(19) arising from the projection onto color antitriplet states. While in ladder approximation the Bethe-Salpeter equations only differ by a factor 2, leading to a weaker binding of diquarks when compared to mesons, beyond ladder approximation these color factors are more significant. The color prefactors of the first and third term in $O(G_D^2)$ are given by $(N_c + 1)/(2N_c)^2 = 1/9$, while for the second term one finds $(N_c + 1)(1 + N_c - N_c^2)/(2N_c)^2 = -5/9$, see Appendix B. Combined with factors arising from the Dirac structure of these terms, the part $\sim -5/9$ is repulsive, giving the possibility to avoid binding, thereby confining the diquarks. It is amusing to note, that for $N_c = 2$, the color factors for mesons and diquarks (which are then colorless “baryons”) are identical up to a minus sign, which is compensated by the different Dirac structure. Unconfined mesons then automatically lead to unconfined diquarks, as expected. In the limit $N_c \rightarrow \infty$ only the repulsive second term of eq. (19), which is of $O(N_c)$, survives (the color prefactor in ladder approximation is given by $-(N_c + 1)/2N_c = -2/3$, i.e. of $O(1)$), which is consistent with Witten’s conjecture [18], stating that mesons are the relevant degrees of freedom for $N_c \rightarrow \infty$. However, in QCD we have neither $N_c = 2$ nor $N_c = \infty$, but $N_c = 3$.

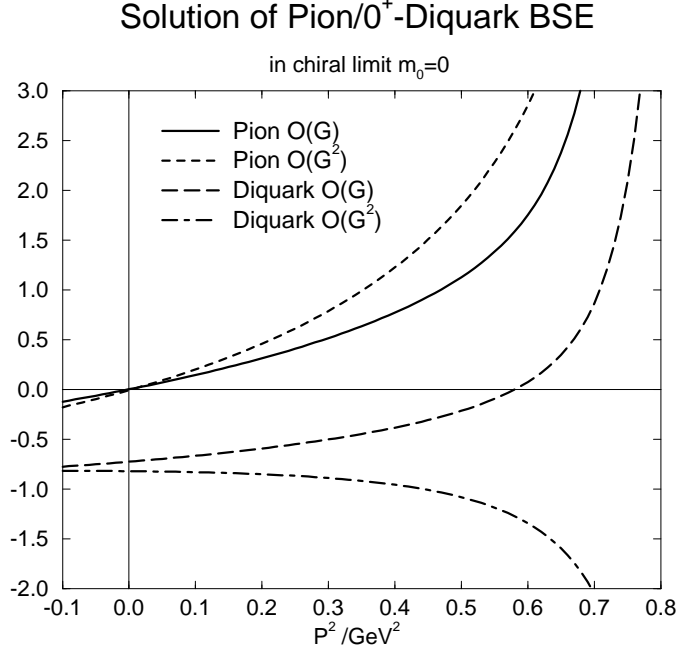


Figure 3: *The inverse of the propagators for the pion and the scalar diquark are shown in ladder ($O(G_{M,D})$) and beyond ladder ($O(G_{M,D}^2)$) approximation in the chiral limit. Its zeros correspond to the squared bound state masses. Scalar diquarks are seen to be confined in $O(G_{0+}^2)$.*

The ansätze of the diquark amplitudes in Dirac space are given by $\Phi_{0+}(P) \simeq \Phi_\pi(P)C$ and $\Phi_{1-}(P) \simeq \Phi_{\rho,\omega}(P)C$, respectively⁴. When inserting these amplitudes into eq. (19), the actual solution of the Bethe-Salpeter equation is obtained in the same manner as for the mesons.

4 Results and Discussions

In this section we present and discuss our numerical results. The bound state masses for the mesons and diquarks in ladder ($O(G_{M,D})$) and beyond ladder ($O(G_{M,D}^2)$) approximation are shown in table (2). As indicated in the previous section, Goldstone's theorem is manifest for the pion; a massless bound state is found in the pseudoscalar channel when the gap equation and the Bethe-Salpeter equation are consistently solved in the same order of $G = G_\pi$ (fig. (3)). When a small current mass is considered in the gap equation, i.e. chiral symmetry is explicitly broken, a finite pion mass is obtained. A comparison of the pion mass in order G_π with the one obtained in order G_π^2 , entails slightly more

⁴ C denotes the charge conjugation matrix, obeying $C\gamma_\mu C^{-1} = -\gamma_\mu^T$. In the Dirac representation it is given by $C = i\gamma^2\gamma^0$.

Solution of Vectormeson/ 1^- -Diquark BSE

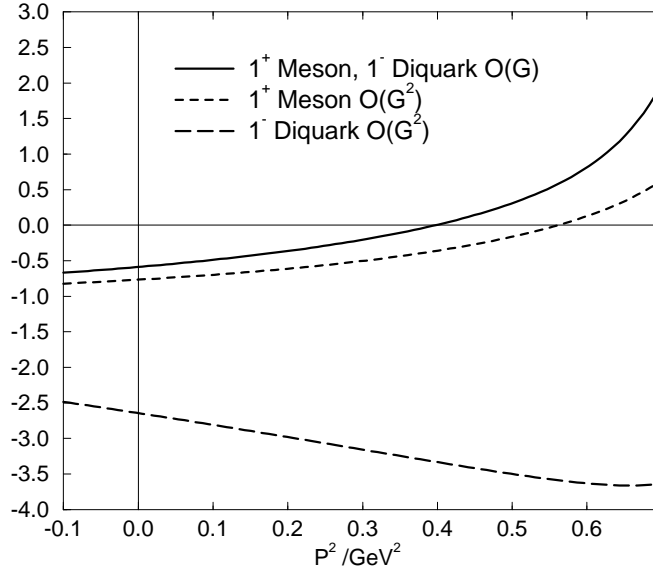


Figure 4: *The inverse of the propagators for the vector meson (1^+) and the axialvector diquark (1^-) is shown in ladder ($O(G_{M,D})$) and beyond ladder ($O(G_{M,D}^2)$) approximation.*

attraction beyond ladder approximation.

For scalar diquarks we obtain the conjectured confinement effect: While to order G_{0+} bound state masses slightly below the pseudothresholds are found, the large repulsive term in the Bethe-Salpeter equation (19) removes the zeros from the inverse of the propagators and therefore confines the scalar diquarks (see fig. (3)). This behaviour is found in the chiral limit as well as in the calculation where a finite current quark mass is considered. We observe furthermore, that the inclusion of the subdominant Bethe-Salpeter amplitude ($\sim \gamma_5 \not{P} C$) is necessary to obtain this feature. Working only with the dominant amplitude leads in $O(G_{0+}^2)$ to scalar diquark masses which, however, lies above the pseudothreshold.

While the pion (and also the scalar diquark) properties are very much dictated by chiral symmetry constraints, the situation is somewhat ambiguous in the vector meson and axialvector diquark channel because there is no symmetry available acting as a guiding principle for detecting the relevant structures. In this respect, we find that the results depend on details of the model, e.g. the ansatz of the amplitude eqs. (14,15) (one might also think of using only γ_μ as the relevant Dirac structure of the amplitude), the values of the coupling constants and even worse, the details of the regularization scheme (see the remark in Appendix A). Our choice of $G_{\rho,\omega} = G$ and $G_{1^-} = 2G$ (leading to equal masses of vector mesons and axialvector diquarks in ladder approximation) and an ansatz of the amplitudes (14), which is ab initio transversal to the total momentum allows at least a

	Bound state mass in $O(G_{M,D})$		Bound state mass in $O(G_{M,D}^2)$	
Quark Mass	$M = 0.3873$	$M = 0.40$	$M = 0.4194$	$M = 0.4295$
Pion	0	0.207	0	0.182
0^+ Diquark	0.762	0.786	unbound	unbound
ρ/ω	0.612	0.630	0.737	0.749
1^- Diquark	0.612	0.630	unbound	unbound

Table 2: *In this table we show the bound state masses of the mesons and diquarks in $O(G_{M,D})$ and $O(G_{M,D}^2)$. We use the parameters indicated in table (1) and values of the coupling constants as explained in the text. The infrared cutoff is fixed to $\mu = 0.1\text{GeV}$. For the diquarks “unbound” means, that the inverse of the propagators has no zero below and slightly above the pseudothreshold $P^2 = 4M^2$, see figure (3), (4).*

qualitatively comparison of vector meson and axialvector diquark properties in $O(G_{M,D}^2)$.

We then find that the vector meson mass in $O(G_{\rho,\omega}^2)$ is about 100 MeV larger than the mass in $O(G_{\rho,\omega})$. For axialvector diquarks the inverse of the propagators has no zero below the pseudothreshold (see fig. 4), but the confining effect is not so clearly seen as in the scalar diquark channel, where the inverse of the propagator (as a function of P^2) to $O(G_{0+}^2)$ will obviously never cross the P^2 -axis, see fig. (3). Here, however, it may be possible, that far above the pseudothreshold a zero of the inverse of the propagator signals a bound diquark state. On the other hand, as mentioned in sect. (2), the model should not be used in the region $P^2 \gg 4M^2$. Nevertheless, also in the axialvector diquark channel the repulsive term in the diquark Bethe-Salpeter equation has a significant effect, which may eliminate the axialvector diquark poles. Due to the absence of tensor mesons (and therefore also tensor diquarks) in the NJL model there is no a priori subdominant Bethe-Salpeter amplitude for axialvector diquarks which could be included in the calculation and which may amplify the confining effect in analogy to the scalar diquark case.

5 Summary and Conclusions

In this paper we investigated, in the context of a NJL model with an infrared cutoff, the conjecture of ref. [10] that diquarks may be confined in a truncation scheme, which is beyond rainbow-ladder approximation. For scalar diquarks we clearly found this feature, due to the color structure a large repulsive part of the Bethe-Salpeter kernel eliminates diquark bound states, whereas in the pion channel, due to different color factors the same term is compensated by attractive parts of the kernel. Vector meson masses are moderately shifted to higher values relatively to their masses obtained in ladder approximation.

For axialvector diquarks it is not possible to answer the question of confinement conclusively, but the observed behaviour also signals severe changes of the inverse diquark propagator in this channel. To conclude, the proposed confinement mechanism for diquarks also work in the NJL model in these channels where the model is suitable: the pion and scalar diquark channel.

It will be interesting to see, if this mechanism of diquark confinement can be confirmed in a calculation including a realistic gluon propagator, thereby “interpolating” between the NJL and the Munczek-Nemirovsky model.

Although the question how and whether diquarks are confined is an interesting question by itself, the outcome of such an investigation has to be included in a baryon calculation, where diquarks enter as effective constituents which are preferably confined. Together with confined quarks such a description leads to baryons which have no quark-diquark thresholds any more [19]. In such an effective diquark-quark model, besides the diquark propagator also the diquark Bethe-Salpeter amplitude enters, which can also be extracted from a diquark calculation presented here or the one of ref. [10].

Acknowledgement We thank L. v. Smekal for helpful discussions and critical reading of the manuscript. Useful comments by H. Weigel are gratefully acknowledged.

A Proper-Time Regularization with an Infrared Cutoff

In order to explicitly demonstrate how the quark confinement mechanism via an infrared cutoff [14] works, we show here the solution of the pion Bethe-Salpeter equation in detail. For simplicity we will restrict ourselves to the ladder approximation and consider only the dominant Bethe-Salpeter amplitude in eq. (13). The Bethe-Salpeter equation (12) then reads

$$\Psi_{\pi 1}(P) = \frac{4}{3} \frac{1}{4} G_{\pi} i \int \frac{d^4 k}{(2\pi)^4} \text{tr} \left[\gamma_{\nu} S(k + \tfrac{1}{2}P) \gamma_5 S(k - \tfrac{1}{2}P) \gamma^{\nu} \gamma_5 \right] \Psi_{\pi 1}(P). \quad (20)$$

Applying the standard techniques for the evaluation of one loop integrals leads, after a Wick rotation, to the expression

$$\Psi_{\pi 1}(P) = \frac{4}{3} G_{\pi} \int_0^1 dx \int \frac{d^4 k_E}{(2\pi)^4} \left[\frac{1}{k_E^2 + M^2} + \frac{(1-x)P^2}{(k_E^2 + Y^2)^2} \right] \Psi_{\pi 1}(P), \quad (21)$$

$$Y^2 = x(x-1)P^2 + M^2. \quad (22)$$

Regularization is performed by using the prescription (7) to obtain

$$\Psi_{\pi 1}(P) = \frac{4}{3} 4G_{\pi} \int_0^1 dx \int_{\frac{1}{\Lambda^2}}^{\frac{1}{\mu^2}} ds \int \frac{d^4 k_E}{(2\pi)^4} \left[\exp(-s(k_E^2 + M^2)) + \left((1-x)P^2 \right) s \exp(-s(k_E^2 + Y^2)) \right] \Psi_{\pi 1}(P). \quad (23)$$

Note that $\mu^2 = 0$ is the usual NJL model expression in proper-time regularization. In eq. (23) the integration over the loop momentum k and over the proper-time s can be done analytically and the final expression (the integration over the Feynman parameter x must be done numerically) for the pion Bethe-Salpeter equation is given by⁵

$$\Psi_{\pi 1}(P) = \frac{1}{16\pi^2} \frac{4}{3} 4M^2 G_{\pi} \left[\left(\Gamma(-1, \frac{M^2}{\Lambda^2}) - \Gamma(-1, \frac{M^2}{\mu^2}) \right) + \frac{P^2}{2M^2} \int_0^1 dx \left(\Gamma(0, \frac{Y^2}{\Lambda^2}) - \Gamma(0, \frac{Y^2}{\mu^2}) \right) \right] \Psi_{\pi 1}(P). \quad (24)$$

Here the s -integrals provided the expressions involving the incomplete Gamma function, e.g., $\Gamma(0, Y^2/\Lambda^2)$ which becomes complex for momenta P^2 larger than the threshold: The solutions of $Y^2 = 0$ for a fixed P^2 are given by

$$x_{1/2} = \frac{1}{2} \pm \sqrt{\frac{1}{4} - \frac{M^2}{P^2}}, \quad (25)$$

i.e. below the threshold at $P^2 = 4M^2$ they are complex and therefore outside of the interval $[0, 1]$, the integration region of the Feynman parameter x . Above threshold, however, we find $Y^2 \leq 0$, for $0 \leq x_1 \leq x \leq x_2 \leq 1$, thereby leading to an imaginary part of the incomplete Gamma function [20],

$$\text{Im} \Gamma(0, \frac{Y^2}{\Lambda^2}) = \pm i\pi |x_2 - x_1| = \pm i\pi \sqrt{(P^2 - 4M^2)/P^2}, \quad (26)$$

displaying the well-known square-root behaviour at the threshold. Since the imaginary part is proportional to $|x_2 - x_1|$ but independent of Λ , it is quite obvious that in the expression

$$\int_0^1 dx \left(\Gamma(0, \frac{Y^2}{\Lambda^2}) - \Gamma(0, \frac{Y^2}{\mu^2}) \right) \quad (27)$$

which appears in eq. (24) the imaginary part arising for $P^2 > 4M^2$ is canceled if μ is kept nonzero.

Although the introduction of an infrared cutoff within the proper-time regularization scheme seems to be a convenient way to avoid unphysical quark thresholds in correlation

⁵When comparing this expression with the first line of the gap equation (9) in the chiral limit one observes the manifestation of Goldstone's theorem.

functions, one must be very careful when applying this scheme in general. In ref. [21] it has been observed that $\Gamma(0, Y^2/\Lambda^2)$ has additional unphysical singularities in the complex P^2 -plane (which is quite obvious, see [20]), located on the imaginary P^2 -axis far beyond the applicability region of the model, $|P^2| < \Lambda^2$. Since their location depends on Λ^2 , they are not canceled by an infrared cutoff. The expression $\Gamma(0, Y^2/\mu^2)$ produces even more unphysical singularities in the correlation function, also located on the imaginary P^2 -axis. Although these singularities play no role if only the Bethe-Salpeter equation is solved, they certainly will affect e.g. formfactor calculations, where a second external momentum can shift the singularities into the physically relevant region of the complex plane. This indicates, that the proper-time regularization with an infrared cutoff must be taken with great care.

Furthermore, we want to add the following remark: Although the proper-time regularization scheme is an unambiguous prescription when applied within a bosonization approach[22] where the fermion determinant is regularized, there are certain ambiguities if the method is used on the level of Feynman diagrams⁶. These ambiguities are connected with various momentum shifts during the calculation. Since this problem does not arise in the gap equation (9), in the pion (and scalar diquark) channel one usually does the calculation in a way, which leads to an analytic manifestation of Goldstone's theorem. However, in the vector meson (and axialvector diquark) channel, chiral symmetry can not be used to resolve the ambiguities. Therefore the results in these channels are not unambiguous.

B N_c -counting beyond ladder approximation

In the meson and diquark Bethe-Salpeter equations different color factors arise which in turn lead to the differences in meson and diquark channels. In color space, the meson Bethe-Salpeter (12) equation can be denoted by

$$\varphi_{jk}^M = (\varphi_L^M)_{li} t_{ij}^a t_{kl}^a + \left((\varphi_1^M)_{li} t_{ij}^a t_{km}^b t_{mn}^a t_{nl}^b + (\varphi_2^M)_{li} t_{im}^b t_{mj}^a t_{kn}^b t_{nl}^a + (\varphi_3^M)_{li} t_{im}^b t_{mn}^a t_{nj}^b t_{kl}^a \right) \quad (28)$$

where the (t^a) are the generators of color $SU(N_c)$. The meson amplitude φ_A^M , ($A = L, 1, 2, 3$, where L denotes the ladder part and $1, 2, 3$ the three terms beyond ladder approximation), describing a color singlet state, is given by the ansatz $\varphi_{ij}^M = \tilde{\varphi}^M \delta_{ij} / \sqrt{N_c}$. Using this ansatz leads to the following color factors:

$$(L) : \frac{1}{N_c} \delta_{li} t_{ij}^a t_{kl}^a \delta_{jk} = \frac{1}{2} \frac{N_c^2 - 1}{N_c}, \quad O(N_c) \quad (29)$$

⁶The usual bosonization approach is deeply connected with the rainbow-ladder approximation and cannot be used in a truncation scheme like the one considered in this paper.

$$(1) : \frac{1}{N_c} \delta_{li} t_{ij}^a t_{km}^b t_{mn}^a t_{nl}^b \delta_{jk} = -\frac{N_c^2 - 1}{4N_c^2}, \quad O(1) \quad (30)$$

$$(2) : \frac{1}{N_c} \delta_{li} t_{im}^b t_{mj}^a t_{kn}^b t_{nl}^a \delta_{jk} = -\frac{N_c^2 - 1}{4N_c^2}, \quad O(1) \quad (31)$$

$$(3) : \frac{1}{N_c} \delta_{li} t_{im}^b t_{mn}^a t_{nj}^b t_{kl}^a \delta_{jk} = -\frac{N_c^2 - 1}{4N_c^2}, \quad O(1), \quad (32)$$

i.e. for $N_c = 3$ the factors appearing in eq.(12) are obtained. In the spirit of an $1/N_c$ -expansion we observe that the term in ladder approximation would be of leading order ($O(N_c)$), while the terms beyond ladder approximation are subleading, ($O(1)$).

The diquark Bethe-Salpeter equation (19) in color space can be written as

$$\varphi_{jk}^D = (\varphi_{L'}^D)_{li} t_{ij}^a t_{lk}^a + \left((\varphi_{1'}^D)_{li} t_{ij}^a t_{mk}^b t_{nm}^a t_{ln}^b + (\varphi_{2'}^D)_{li} t_{im}^b t_{mj}^a t_{nk}^b t_{ln}^a + (\varphi_{3'}^D)_{li} t_{im}^b t_{mn}^a t_{nj}^b t_{lk}^a \right), \quad (33)$$

where the prescription (18) has been used to derive it formally from the meson Bethe-Salpeter equation (note, $(t_{ij}^a)^T = t_{ji}^a$). The projection on color antitriplet diquark states is most conveniently done by using the ansatz $\varphi_{ij}^D = \tilde{\varphi}^D \epsilon_{ij}^a / \sqrt{N_c - 1}$ of the diquark amplitude, involving the normalized Levi-Cevita tensor $\epsilon_{ij}^a / \sqrt{N_c - 1}$. Then the resulting color factors in the diquark channel are given by

$$(L') : \frac{1}{N_c - 1} \epsilon_{li}^c t_{ij}^a t_{lk}^a \epsilon_{jk}^d = -\frac{N_c + 1}{2N_c} \delta^{cd}, \quad O(1) \quad (34)$$

$$(1') : \frac{1}{N_c - 1} \epsilon_{li}^c t_{ij}^a t_{mk}^b t_{nm}^a t_{ln}^b \epsilon_{jk}^d = \frac{N_c + 1}{(2N_c)^2} \delta^{cd}, \quad O(1/N_c) \quad (35)$$

$$(2') : \frac{1}{N_c - 1} \epsilon_{li}^c t_{im}^b t_{mj}^a t_{nk}^b t_{ln}^a \epsilon_{jk}^d = \frac{N_c + 1}{(2N_c)^2} (1 + N_c - N_c^2) \delta^{cd}, \quad O(N_c) \quad (36)$$

$$(3') : \frac{1}{N_c - 1} \epsilon_{li}^c t_{im}^b t_{mn}^a t_{nj}^b t_{lk}^a \epsilon_{jk}^d = \frac{N_c + 1}{(2N_c)^2} \delta^{cd}, \quad O(1/N_c). \quad (37)$$

For the case $N_c = 3$ we obtain the color factors appearing in eq.(19). As mentioned in section(3), the different terms in the diquark channel shows a rather interesting $N_c \rightarrow \infty$ behaviour. In leading order one would just keep the term (2') which is of $O(N_c)$. However, the whole contribution of this term in the diquark Bethe-Salpeter equation is repulsive and thereby eliminates diquarks totally. The attractive ladder part of the Bethe-Salpeter equation contributes in this scheme only in subleading order, $O(1)$, and the attractive terms beyond ladder approximation only in order $O(1/N_c)$.

References

- [1] Y. Nambu and G. Jona-Lasinio, Phys. Rev. **122**, 345 (1961).
- [2] P. C. Tandy, “Hadron Physics from the Global Color Model of QCD”, e-print nucl-th/9705018, to appear in Prog. Part. Nucl. Phys. **39**, 1997.
- [3] R. Alkofer, H. Reinhardt, and H. Weigel, Phys. Rep. **265**, 139 (1996);
C. V. Christov et al., Prog. Part. Nucl. Phys. **37**, 1 (1996).
- [4] M. R. Frank, P. C. Tandy and G. Fai, Phys. Rev. **C43**, 2808 (1991).
- [5] R. T. Cahill, Austr. J. Phys. **42**, 171 (1989).
- [6] H. Reinhardt, Phys. Lett. **B244**, 316 (1990).
- [7] U. Zückert, R. Alkofer, H. Weigel, and H. Reinhardt, Phys. Rev. **C55**, 2030 (1997).
- [8] Proceedings of the Conference *Diquarks 3*, Torino, Oct. 28-30, 1996; eds.: M. Anselmino and E. Predazzi, to be published by World Scientific.
- [9] R. T. Cahill and C. D. Roberts, Phys. Rev. **D36**, 2804 (1987).
- [10] A. Bender, C. D. Roberts, and L. v. Smekal, Phys. Lett. **B380**, 7 (1996).
- [11] H. J. Munczek and A. M. Nemirovsky, Phys. Rev. **D28**, 181 (1983).
- [12] L. v. Smekal, A. Hauck and R. Alkofer, “The Infrared Behaviour of Gluon and Ghost Propagators in Landau Gauge QCD”, e-print hep-ph/9705242.
- [13] C. D. Roberts and A. G. Williams, Prog. Part. Nucl. Phys. **33**, 477 (1994).
- [14] D. Ebert, T. Feldmann and H. Reinhardt, Phys. Lett. **B388**, 154 (1996).
- [15] C. Weiss, A. Buck, R. Alkofer and H. Reinhardt, Phys. Lett. **B 312** (1993) 6.
- [16] C. J. Burden, L. Qian, C. D. Roberts, P. C. Tandy and M. J. Thompson, Phys. Rev. **C 55**(1997), 2649.
- [17] G. Hellstern, Ph.D. Thesis, Tübingen University; in preparation.
- [18] E. Witten, Nucl. Phys. **B160**, 57 (1979).
- [19] G. Hellstern, R. Alkofer, M. Oettel and H. Reinhardt, “Nucleon form factors in a covariant diquark-quark model”, e-print hep-ph/9705267.
- [20] M. Abramowitz and I. A. Stegun, Handbook of Mathematical Functions, Dover, New York, 1965.
- [21] W. Broniowski, G. Ripka, E. Nikolov and K. Goeke, Z. Phys. **A354**(1996), 421.
- [22] D. Ebert and H. Reinhardt, Nucl. Phys. **B271**, 188 (1986).